Theor Chim Acta (1996) 94: 13–22

Theoretica Chimica Acta

AM1 study of Wolff and 1,2-hydrogen shift rearrangements of β-oxy-α-Diazo carbonyl compounds

F. Enríquez[1], F.J. López-Herrera[2], J.J. Quirante[1], F. Sarabia[2]

[1] Departamento de Química Fisica, [2] Departamento de Bioquímica, Biología Molecular y Química Orgánica, Facultad de Ciencias, E-29071 Málaga, Spain

Received December 9, 1995/Accepted January 18, 1996

Abstract. The study of several thermal processes involved in the β-oxy-α-diazo carbonyl compounds chemistry at the AM1 semiempirical level is reported. Principally, our study focussed on competitive Wolff and 1,2-hydride rearrangement reactions involving nitrogen elimination that a particular type of β-oxy-α-diazo carbonyl compounds (see scheme 1) can undergo under certain conditions. The AM1 results provide a reasonable description of the energy-related and structural aspects involved in the elementary processes considered.

Key words: AM1 – Wolff Rearrangement – β-Oxy-α-Diazo carbonyl compounds

1 Introduction

A previous comprehensive experimental study [1, 2] aimed at finding new asymmetric synthetic pathways for 1-methyl-2-hydroxy units with a view to the preparation of a variety of compounds of interest (e.g. macrolide antibiotics) was completed in this work by carrying out a semiempirical quantum chemical study of some elementary processes involved in a new, recently developed synthetic scheme [2]. The scheme involves aldol condensation reactions between chiral aldehydes (e.g. 2,3-O-isopropylidene-D-glyceraldehyde) and diazo ketones to form a β-oxy-α-diazo carbonyl compound (DK in Scheme 1). Specifically, our study focussed on potential Wolff rearrangement (WR) and 1,2-hydride rearrangement reactions involving nitrogen elimination that DK can undergo under certain conditions.

Even though the chemistry of Wolff rearrangement has been widely studied in many respects, its mechanism has been the subject of much debate and of both theoretical and experimental research. Authors argue whether nitrogen elimination and the 1,2 migration of the carbon atom take place in a concerted or stepwise manner and, in the latter case, whether the precursor for the ketene (KE) is the ketocarbene (KC) or an oxyrene intermediate (OX). Experimental evidence suggests that they all may depend on the particular α-diazo ketone [3–6]; thus, some WR processes allow one to rule out the involvement of the ketocarbene [4, 5] and others (e.g. those of cyclic diazo ketones) that of the oxyrene [6]. In any case, there

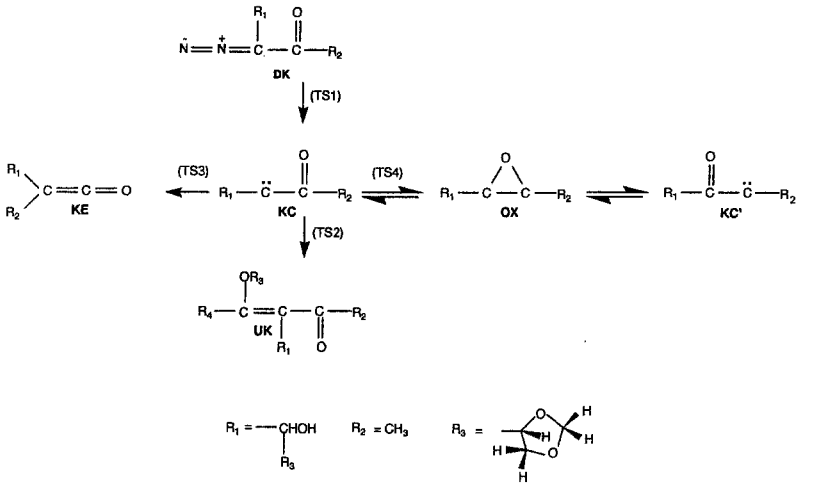

Scheme 1

seems to be general consensus that the first step in WR is the formation of the ketocarbene (KC in Scheme 1) [7], whose involvement in the process has been widely documented [7–15] (e.g. by ESR of the triplet state produced by photochemical induction [7–13]). The carbene can envolve to the ketene (KE) or, R1 providing, to an α,β-unsaturated ketone (UK). Isomerization via the oxyrene (OX) has also been observed in experiments with asymmetrically substituted [16] and isotope labelled α-diazo ketones [17–19].

For theoretical studies based on the potential hypersurface model to lead to reliable conclusions, computations must be carried out with an appropriate quantum chemical method and using full optimization throughout the entire coordinate system space while avoiding constraints that might condition the results. Highly theoretical *ab initio* studies carried out on the simplest possible system (R1 = R2 = H) [20–24] have provided interesting information on potential energy hypersurfaces for the ground state [24] and, in some cases, excited states [22, 23]. Thus, Novoa et al. [22] used MC-SCF gradient optimization techniques at the 6-31G* level to study the interconversion between the ketocarbene (KC) and the oxyrene (OX), as well as the region where the surfaces for the single and triplet state intercept; they demonstrated the role that the triplet state of the oxyrene may play in WR reactions. Yoshimine [23] used MC-SCF and MRCI methods to investigate the interconversion between ketene (KE) and its isomer oxyranylidene. Some reactivity studies based on semiempirical methods (MNDO, MNDO/C [25–27] and MINDO/3 [28, 29]) have also been reported for this and related systems, all involving the ground state. Schröder and Thiel [25, 26] showed MNDO methods and their correlated versions, MNDO/C, to be consistent with more expensive *ab initio* computational methods as regards the number and type of stationary points for the $C_2H_2ON_2$ system, and to lead to acceptable geometries relative to the reference *ab initio* calculations; the non-correlated version, however, provides more divergent results as regards energies.

In some *ab initio* studies of the elementary processes of Scheme 1 in the triplet state (that with the lowest energy in the carbene), activation energy barriers were found very high relative to those calculated for the lowest ground state [20]. Unsurprising, many studies on WR suggest potential intersystem crossing as

part of the overall mechanism; consequently, all semiempirical calculations on WR were limited to the potential energy hypersurface (PES) for the lowest-energy singlet state.

This paper reports the results obtained by applying the AM1 semiempirical method to the thermal processes of Scheme 1. We used a semiempirical method owing to the large number of atoms involved in the system studied, and AM1 in particular as it had previously proved to clearly surpass their predecessors (MINDO/3 and MNDO) in reactivity studies.

2 Computational method

Calculations were carried out using the AM1 (Austin Model 1) method [30] as implemented in v. 6.0 of the programme MOPAC [31]. The 'PRECISE' option was always included in the data file in order to increase convergence criteria by default by a factor of (usually) 100.

Full optimization throughout the coordinate space was carried out, unrestrictedly, to energy gradient norm values below 0.1 kcal/mol for every stationary point (equilibrium minima, transition states, ...) on the PES. For this purpose, pertinent options for each point type in MOPAC were used. The topological nature of the different points located was finally determined from frequencies and force constants.

3 Results and discussion

In this work we characterized the minima for the reactant (DK) and the intermediates of Scheme 1 (KC and OX) in the lowest-energy PES, as well as the transition states for each elementary process between them and with the different reaction products. Species such as those in Scheme 2 are also KC isomers, as shown in some theoretical studies [20, 21, 23, 25] – the KC interconversion barriers in such structures were very high, however, so they were not considered in this study.

Table 1 lists the most salient geometric parameters for each point; their optimized structures are shown in Fig. 1 (transition states include the atomic components of the transition vector).

TS1 is the transition state for the thermal elimination of molecular nitrogen from DK to yield the corresponding ketocarbene (KC). The length of the N_{22}–C_3 bond at that point has expanded to 2.0 Å. On the other hand, the C_2–C_3 and C_3–C_4 bonds become virtually of the same length, as in the KC molecule. Eliminating N_2 brings about dramatic conformational changes in the acyclic portion of the system (as reflected in the dihedral angles given in Table 1), since the process involves the loss of conjugation in the molecular portion comprising atoms N_{23},

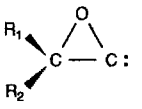

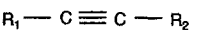

Scheme 2

Table 1. Values calculated for several geometric parameters of the stationary points of the AM1 ground potential energy hypersurface

	DK	TS1	KC	TS2	TS3	TS4	OX	TS5
	BONDS LENGTHS (Å)							
C_1–C_2	1.494	1.495	1.503	1.502	1.792	1.457	1.437	1.497
C_1–C_3	2.549	2.536	2.441	2.455	2.032	2.631	2.710	2.522
C_2–C_3	1.468	1.446	1.416	1.399	1.302	1.315	1.299	1.502
C_3–C_4	1.512	1.463	1.440	1.365	1.436	1.435	1.455	1.441
C_2–O_{10}	1.242	1.249	1.246	1.247	1.215	1.335	1.456	1.234
C_3–O_{10}						1.826	1.467	2.409
H_{15}–C_3	2.129	2.027	2.073	1.496	2.060	2.091	2.130	1.316
H_{15}–C_4	1.130	1.143	1.140	1.310	1.136	1.135	1.130	1.486
N_{22}–C_3	1.325	2.000	∞	—	—	—	—	1.496
N_{23}–N_{22}	1.128	1.108	—	—	—	—	—	1.126
	BONDS ANGLES (Degrees)							
C_1–C_2–C_3	118.7	119.2	113.5	115.6	80.4	143.2	164.0	114.5
C_1–C_2–O_{10}	121.8	121.2	122.2	121.7	118.4	129.7	131.9	122.3
C_2–C_3–O_{10}						46.9	63.2	
C_3–C_2–O_{10}						87.13	64.0	
C_2–C_3–N_{22}	121.9	110.1	—	—	—	—	—	112.7
C_4–C_3–N_{22}	121.5	112.1	—	—	—	—	—	118.0
C_2–C_3–C_4	116.6	122.4	135.1	152.5	156.3	168.5	166.9	117.1
C_3–C_4–H_{15}	106.5	101.4	106.4	68.0	105.8	108.3	110.3	53.4
C_4–C_3–H_{15}	—	—	—	54.3	—	—	—	65.0
C_3–C_4–O_{11}	110.5	115.5	116.0	124.5	112.1	112.9	111.5	116.3
C_3–C_4–C_5	115.1	116.8	110.0	121.3	115.0	111.0	110.7	123.5

DIHEDRAL ANGLES (Degrees)								
C_1–C_2–C_3–C_4	−173.6	119.9	−97.9	−99.2	−95.7	163.6	−17.9	78.5
C_4–C_3–C_2–O_{10}	6.3	−66.0	89.9	86.1	108.1	−16.8	168.0	−104.9
C_2–C_3–N_{22}–N_{23}	−167.1	−116.2	—	—	—	—	—	125.4
C_4–C_3–N_{22}–N_{23}	12.35	103.88	—	—	—	—	—	−93.3
C_2–C_3–C_4–H_{15}	53.3	98.4	−128.1	−99.1	87.7	−152.8	−12.8	−98.2
H_{15}–C_4–C_3–N_{22}	−126.3	−127.4	—	—	—	—	—	122.2
O_{10}–C_2–C_3–N_{22}	−174.2	159.1	—	—	—	—	—	36.8
O_{11}–C_4–C_3–N_{22}	114.5	114.3	—	—	—	—	—	37.3
C_3–C_4–O_{11}–H_{16}	60.4	53.7	−62.4	−7.1	42.4	−52.5	−45.9	158.3
C_2–C_3–C_4–C_5	175.0	−144.0	−128.1	−165.0	32.9	−32.6	108.4	19.2
C_3–C_4–C_5–O_9	−56.4	−57.0	−81.8	−129.6	−66.4			
C_3–C_2–C_1–H_{12}	178.5	−170.6	148.5	160.9	−123.8	146.2	178.8	62.9
C_3–C_2–C_1–H_{13}	58.8	70.4	27.5	39.9	120.2	25.14	58.4	−57.0
C_3–C_2–C_1–H_{14}	−61.8	−50.3	−92.9	−80.3	−2.9	−94.8	−61.2	−177.5
C_3–C_4–C_5–C_6	−172.6	−172.9	162.2	113.9	177.5	164.6	170.7	83.7

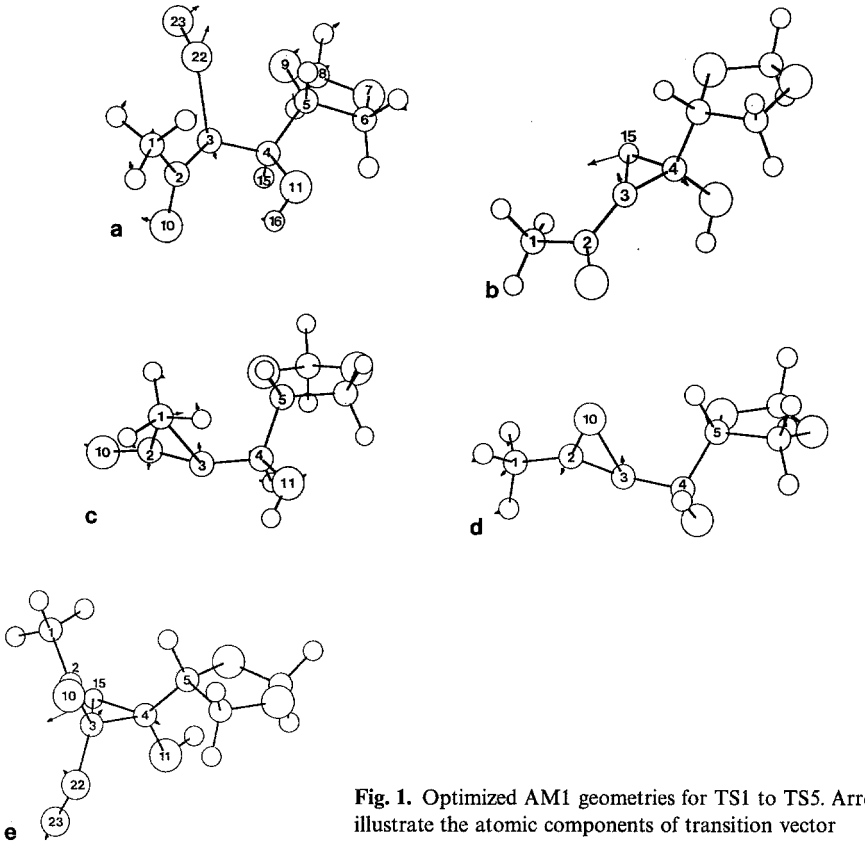

Fig. 1. Optimized AM1 geometries for TS1 to TS5. Arrows illustrate the atomic components of transition vector

N_{22}, C_3, C_2 and O_{10}, which is responsible for the initial planarity of the acyclic chain in DK. Different values for C_2–C_3 and C_3–C_4 bonds lengths in DK is also consequence of this conjugation. As can be seen in Fig. 1a, the two fragments that are formed depart in such a way that the nitrogen–nitrogen bond remains parallel to the plane defined by sites C_2, C_3 and C_4. One other geometric change involved in this step is the opening by ca. 5° of the bond angle defined by atoms C_3, C_4 and O_{11}, which is very close to that of the ketocarbene in the transition state.

The geometry obtained for the carbene (KC) has the C_2–C_1 and C_4–H_{15} bonds virtually aligned with orbital Pz in C_3, which is vacant in the singlet state considered for the carbene. Hence, it is appropriately arranged for the migration of H_{15} or that of the methyl group at C_2. TS2 and TS3 (Fig. 1b and c, respectively) are the transition states, in that order, for such mutually competitive elementary processes, viz. that giving the corresponding α,β-unsaturated ketone (UK) and that yielding the Wolff rearrangement product (the ketene, KE).

Both transition states correspond to non-planar geometries as regards the atoms that are directly involved in the two processes; the most significant dihedral angles defined by such atoms ($C_1C_2C_3C_4$, $C_4C_3C_2O_{10}$ and $H_{15}C_4C_3C_2$) are close to 90° at TS2 and TS3, which again confirms that the starting conformation assumed for species KC is the most suitable as it prefigures that of the corresponding transitions states. In this respect, the AM1 predictions are quite consistent with

those of the more recent high-level *ab initio* calculation methods for Wolff rearrangement mechanism [24].

Depending on the reaction pathway the system takes, the supermolecule portion not including the reaction domain (atoms C_1, C_2 and C_3 in one case, and H_{15}, C_4 and C_3 in the other) rotates freely about appropriate bonds to adopt the arrangement resulting in the most stable transition state possible. Thus, in TS2, a projection along the C_5–C_4 bond, reveals that the other three bonds lie in a virtually alternate arrangement (including the H_{15}–C_4 bond, which is in the process of breaking) that encompasses C_4 and C_5. In TS2, the five-centre cyclic residue is rather differently arranged; this is the configuration leading to the least steric interaction between such a group and a methyl group, the displacement of which along the reaction coordinate results in an approach to the cyclic residue.

We also calculated TS4 (Fig. 1d), viz. the transition state for the isomerization of the ketocarbene (KC) to the oxyrene (OX). The intermediate character of OX has been demonstrated experimentally in many ways (for example, by studying the isomerization of ketocarbenes with different substituents or others isotopically labelled at C_2 and C_3 [16–19]). Also, oxyrenes seemingly play a more prominent role in the thermolysis of diazo ketones at high temperatures [24], which is ascribed to a higher stability of the corresponding ketocarbene. The oxyrene isomer of the prototype system C_2H_2O has been widely studied theoretically [21, 24]. Significant differences between the geometric predictions (essentially lengthened C–O and C–C distances) of various types of *ab initio* calculations are obtained when electronic correlation is considered (by using any available method such as MP2, CCSD, etc.); less marked differences have also been encountered in terms of the number of base functions used. The AM1 results for OX are quite consistent (0.03 Å default for C–O bonds, and 0.02 Å in excess for the C–C ones) with the best *ab initio* calculations – correlated at the CCSD(T) level with massive bases – of Radom and Shaefer III [24], which are repeatedly mentioned in our discussions as they are the latest available to us.

The AM1 geometry for the transition state of the elementary process KC → OX (TS4) is also highly consistent with that predicted by various *ab initio* calculations; however, *ab initio* results for such a point are controversial since, while most predict its existence as a true transition state, calculations MP2/6-311G(*df*, *p*) failed to locate the corresponding saddle point and CCSD(T)/6-311G(*d*, *p*) or density functional calculations [24] suggested that the OX-like structure is a saddle point. The most recent calculations [24] for the TS4 analogue, obtained by Radom and Shaefer III with analytical optimization of the gradient at the RHF level, density functional theory, MP2 and coupled cluster treatment, revealed this geometry (particularly the C_2–O_{10} and C_3–O_{10} bond distances) to be very sensitive to the inclusion of electronic correlation in the calculations (it shortens O_{10}–C_3 and lengthens O_{10}–C_2) and somewhat less sensitive to the use of increasingly large basis sets, which have the opposite effect on the interatomic distances between the oxygen and the two carbon atoms. The C_2–C_3 bond hardly varies with the type of calculation. The AM1 value for the shorter C–O bond in TS4, 1.335 Å, is very close to those derived from *ab initio* calculations by other authors [21, 22], particularly that obtained by Radom and Shaefer III (1.383 Å) using their best treatment; also, the AM1 value for the longer bond, 1.826 Å, was 0.2 Å longer than that of Radom and Shaefer III, i.e. much closer than those obtained by Bouma et al. with optimization at the RHF/4-31G (1.918 Å) or by Novoa from MC-SCF 6-31G* calculations (2.39 Å).

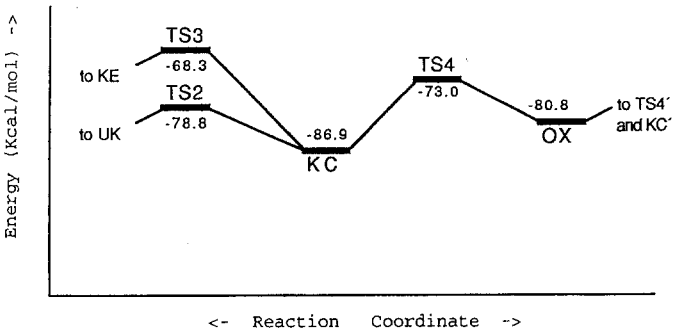

Fig. 2. Energy profiles for the processes considered. Energy is the standard heat of formation, in kcal/mol

Table 2. Heat of formation (kcal/mol), dipolar moment (D) and net charges (−e) for stationary points calculated

	DK	TS1	KC	TS2	TS3	TS4	OX	TS5
ΔH_f^0	−114.51	−64.67	−86.93	−78.79	−68.29	−73.00	−80.84	−56.69
μ	2.295	1.804	2.363	3.255	2.309	1.814	1.822	3.831
qC_1	−0.271	−0.255	−0.253	−0.259	−0.290	−0.197	−0.140	−0.276
qC_2	0.303	0.191	0.211	0.295	0.317	0.227	0.026	0.234
qC_3	−0.384	−0.063	−0.083	−0.392	−0.305	−0.191	−0.096	−0.194
qC_4	0.098	−0.012	−0.003	0.165	0.126	0.128	0.123	−0.112
qO_{10}	−0.319	−0.334	−0.329	−0.341	−0.273	−0.377	−0.290	−0.271
qO_{11}	−0.335	−0.343	−0.335	−0.300	−0.333	−0.317	−0.312	−0.261
qN_{22}	0.205	0.049	—	—	—	—	—	0.075
qN_{23}	0.022	0.040	—	—	—	—	—	−0.036
qH_{15}	0.128	0.149	0.188	0.179	0.130	0.168	0.146	0.249

Figure 2 depicts schematically the energy aspects of the different reactions studied (see also Table 2). As regards the relative stabilities of KC and OX, our results, as expected, revealed the acyclic ketocarbene (KC) to be ca. 6 kcal/mol more stable. The calculated activation energies for the direct isomerization (KC → OX) and inverse isomerization (OX → KC) were 13.9 and 7.8 kcal/mol. Those for the competitive processes were 18.6 kcal/mol (KC → KE) and 8.1 kcal/mol (KC → UK), respectively; therefore, H migration is the most favourable choice for KC evolution. On the other hand, the conversion of KC into OX via TS4 is more favourable than the formation of the ketene (KE) via TS3; this AM1 prediction is consistent with those of the best *ab initio* results [24]. We may therefore conclude that the semiempirical method used successfully predicts the existence of every transition state on the potential energy surface of the system, and in close agreement with the most elaborate *ab initio* calculations using full geometry optimization; in addition, it also predicts relative stabilities and, despite the difference between the system studied in this work and the reference prototype for which all *ab initio* calculations are available (C_2H_2O), it is a good approximation to the activation energies of the processes involved.

We also located a saddle point connecting the minima for DK and UK + N_2 (TS5) in the potential energy hypersurface and hence corresponding to the transition state for a process where 1,2 hydrogen migration and nitrogen elimination take place simultaneously in a concerted manner from DK (Fig. 1e). At such a point, the N_{22}–C_3 bond length is 1.496 Å and thus much shorter than at TS1. This option has an associated activation enthalpy of 57.87 kcal/mol. However, based on our results, the rate-determining step in the stepwise process (DK → KC + N_2 → UK + N_2) is the first step, i.e. the elimination of nitrogen; therefore, the activation energy for the overall reaction is 49.84 kcal/mol, so the stepwise mechanism is the choice with the lowest energy demands, but not the only one.

Several attempts at finding a similar transition state for the concerted process DK → KE + N_2 failed. Low-dimensional surfaces obtained by using the reaction coordinate technique to plot the supermolecule energy as a function of the two geometric parameters which, to the author's minds may contribute maximally to the true coordinate of the hypothetical concerted pathway (viz. the C_3–C_1 and C_3–N_{22} interatomic distances), allowed us to rule out the existence of a transition state connecting the minima for DK and KE; in fact, the sole route connecting such minima in the calculated surfaces was that passing by KC (i.e. that for the stepwise mechanism). Nor could we locate a saddle point such as that obtained by Tsuda et al. using MINDO/3 [28, 29] for $C_2H_2ON_2$ in a process involving the concerted elimination of molecular nitrogen and the cyclization of the supermolecule to form oxyrene. We used AM1 to study the potential hypersurface for the previous reaction and failed to locate the above-mentioned saddle point. We can therefore assume that the MINDO/3 predictions may have been affected by the excessive artificial stability introduced by its calculations for species including small rings [32].

It should be noted that the AM1 energies for TS1 and TS5 (viz. the transition states involving the formation of an N_2 molecule), may have been overestimated by about 10 kcal/mol as a result of the error with which AM1 predicts the formation enthalpy of the nitrogen molecule (11.17 kcal/mol vs. the experimental 0.0 kcal/mol), so the barriers for the corresponding reactions may have been overestimated by ca. 10 kcal/mol. For this reason, the energies predicted by AM1 for processes involving N_2 elimination should be used reservedly. From a comprehensive experimental and theoretical study (MINDO-BWEN on the hypersurface of the lowest-energy singlet state) of the photolysis of various α-diazo ketones (some cyclic), Bachman et al. [3c] showed the activation barriers for the different processes included in Scheme 1 to depend on the nature of R1 and R2 (and R3): the KE/UK ratio or the ability to experimentally detect OX depends on the nature of such groups. For this reason, we avoided comparing our AM1 activation energies with those experimentally or theoretically determined for related systems such as H_2C_2O.

On the other hand, based on our activation energies for the two competitive processes, KC → KE and KC → UK, the experimental UK/KC ratio for a gas-phase reaction conducted at a low pressure should be infinity. The experimental results available [33] for the system studied correspond to the photochemical reaction induced by irradiating DK in methanol with monochromatic light of 253.7 nm (photon energy ca. 60 kcal/mol), which yielded UK quantitatively (100%). Under these conditions, the substitution of H_{16} by protective groups of a different electronic character decreased the KE/UK ratio to values below unity in some instances. In any case, any correlations between the calculated activation

barriers and experimentally observed KE/UK ratios are not immediate. The KE/UK ratio in these reactions has been widely shown to depend on additional factors such as the way the process is induced, the solvent and, with photo-induced reactions, whether a rapid vibrational relaxation of the ketocarbene is possible [32] (KC, which is usually formed with a large excess of vibrational energy).

References

1. López Herrera FJ, Sarabia F (1993) Tetrahedron Lett 34:3467
2. López Herrera FJ, Sarabia F (1994) Tetrahedron Lett 35:2929
3. a) Nguyen MT, Hajnal MR, Ha T, Vanquickenborne LG, Wentrup C (1992) J Am Chem Soc 114:4387; b) Nguyen MT, Hajnal MR, Vanquickenborne LG (1994) J Chem Soc Perkin Trans II 169; c) Bachmann C, N'Guessan TY, Debû F, Monnier M, Pourcin J, Aycard JP, Bodot H (1990) J Am Chem Soc 112:7488
4. Tanigaki K, Ebbesen TW (1987) J Am Chem Soc 109:5883
5. Tanigaki K, Ebbesen TW (1989) J Phys Chem 93:4531; and references therein
6. a) Zeller KP (1975) J Chem Soc Chem Commun 317; b) Majerski Z, Redvanly CS (1972) J Chem Soc Chem Commun 694; c) Timm U, Zeller KP, Meier H (1977) Tetrahedron 33:453
7. Torres M, Ribo J, Chement A, Strausz OP (1983) Can J Chem 61:996
8. Murai H, Shafarik I, Torres M, Strausz OP (1988) J Am Chem Soc 110:1025
9. Murai H, Ribo J, Torres M, Strausz OP (1981) J Am Chem Soc 103:6422
10. Tomioka H, Okuno H, Izawa Y (1980) J Org Chem 45:5278
11. Torres M, Raghunathan P, Bourdelande JL, Chement A, Toth G, Strausz OP (1986) Chem Phys Lett 127:205
12. Moriconi EJ, Murray JJ (1964) J Org Chem 29:3577
13. Murai H, Torres M, Ribo J, Strausz OP (1983) Chem Phys Lett 101:202
14. McMahon RJ, Chapman OL, Hayes RA, Hess TC, Krimmer HP (1985) J Am Chem Soc 107:7597
15. Hayes RA, Hess TC, McMahon RJ, Chapman OL (1985) J Am Chem Soc 107:7597
16. Matlin SA, Sammes PG (1972) J Chem Soc Perkin Trans 1:2623
17. Zeller KP, Meier H, Kolshorn H, Muller E (1972) Chem Ber 105:1875
18. Zeller KP (1977) Tetrahedron Lett 707
19. a) Frater G, Strausz OP (1970) J Am Chem Soc 92:6654; b) Thornton DE, Gosavi RK, Strausz OP (1970) J Am Chem Soc 92:1768; c) Csizmadia IG, Front J, Strausz OP (1968) J Am Chem Soc 90:7360
20. Tanaka K, Yoshimine M (1980) J Am Chem Soc 102:7655
21. Bouma WJ, Nobes RH, Radom L, Woodward CL (1982) J Org Chem 47:1869
22. Novoa JJ, McDouall JJW, Robb MA (1987) J Chem Soc Faraday Trans II, 83:1629
23. Yoshimine M (1989) J Chem Phys 90:378
24. Scott AP, Nobes RH, Schaefer HF III, Radom L (1994) J Am Chem Soc 116:10 159 and references therein
25. Schröder S, Thiel W (1985) J Am Chem Soc 107:4422
26. Schröder S, Thiel W (1986) J Am Chem Soc 108:7985
27. Reference 3c and references therein
28. Tsuda M, Oikawa S, Nagayama N (1987) Chem Pharm Bull 35:1
29. Tsuda M, Oikawa S (1989) Chem Pharm Bull 37:1
30. Dewar MJS, Zoebish EG, Healy EF, Stewart JJP (1985) J Am Chem Soc 107:3902
31. Stewart JJP (1983) QCPE 3:43
32. McManus SP, Smith MR (1978) Tetrahedron Lett 22:1897
33. Sarabia F (1994) Thesis Universidad de Málaga, Málaga